Journal of Power Sources 186 (2009) 557–564

Contents lists available at ScienceDirect

Journal of Power Sources

journal homepage: www.elsevier.com/locate/jpowsour

Electrophoretic deposition of nickel oxide electrode for high-rate electrochemical capacitors

Mao-Sung Wu*, Chen-Yu Huang, Kun-Hao Lin

Department of Chemical and Materials Engineering, National Kaohsiung University of Applied Sciences, Kaohsiung 807, Taiwan, ROC

ARTICLE INFO

Article history:
Received 22 March 2008
Received in revised form 2 October 2008
Accepted 8 October 2008
Available online 22 October 2008

Keywords:
Electrophoretic deposition
Nickel oxide electrode
Nanoplatelets
Porous thin film
Electrochemical capacitors

ABSTRACT

Nanostructured nickel hydroxide electrode is fabricated directly by electrophoretic deposition (EPD) method. After annealing at 300 °C for 3 h, nickel hydroxide nanoplatelet converts into nickel oxide. EPD method is useful in depositing nickel hydroxide nanoplatelets from isopropyl alcohol suspension containing iodine and water additives. Hydrogen ions are generated by the reaction between iodine and water and then adsorbed on the nickel hydroxide, resulting in positively charged nickel hydroxide. Positively charged nanoplatelet of high zeta potential is beneficial to EPD and dispersion. An electrode deposited by EPD has better uniformity than one deposited by dip coating. Electrochemical performance of the electrodes is investigated by cyclic voltammetry in 0.5 M KOH. Specific capacitance of the nickel oxide electrode prepared by EPD is higher than that of prepared by dip coating even at a very high rate of 500 mV s^{-1}. In addition, an electrode prepared by EPD also shows excellent cycle-life stability because its specific capacitance decreases only slightly after 5000 charging/discharging cycles.

1. Introduction

Recently, nickel oxides have been intensively studied due to their potential applications in electrochromic films, optical materials, fuel cell electrodes, photocatalysts, and electrochemical capacitors, etc. Due to the high power demand of portable electronic devices and electric vehicles, electrochemical capacitors that deliver higher power density than traditional batteries have been investigated extensively in recent years. Transition metal oxides such as ruthenium oxides, manganese oxides, and nickel oxides have been demonstrated to be the electrode materials for electrochemical capacitors owing to their higher specific capacitances. Among these oxides, a hydrous form of ruthenium oxide in aqueous H_2SO_4 possesses a high specific capacitance of 720 F g^{-1} at a low scan rate of 2 mV s^{-1} and an excellent cycle-life stability [1,2]. However, a disadvantage of ruthenium oxide is that it is too expensive for commercial use. Most of the researches are, therefore, focused on alternative electrode materials that are inexpensive and exhibit capacitive behavior comparable to that of ruthenium oxide.

Generally, nickel oxides are prepared by thermal treatment of the nickel hydroxides for electrochemical capacitors. Nickel hydroxide oxide materials have been widely used for the positive electrode in rechargeable alkaline batteries such as nickel–cadmium and nickel–metal hydride batteries. For fabricating nickel oxide electrodes, several techniques such as slurry coating [3], dip coating [4], and electrochemical deposition [5–11] have been reported to be the possible manufacturing processes for electrochemical capacitors. Electrophoretic deposition (EPD) of the nickel oxide electrode has rarely been studied, especially for electrochemical capacitors. More recently, the high-power density supercapacitor electrodes of carbon nanotube films prepared by EPD have been reported [12,13]. Also, EPD of hydrous ruthenium oxides with polytetrafluoroethylene (PTFE) and their supercapacitor performances have been investigated systematically as a high-power capacitor [14,15]. To the best of our knowledge, EPD of the nickel oxide electrode for electrochemical capacitors has not been reported earlier, especially for high-rate applications.

Some of the fabrication methods, such as slurry coating and dip coating, suffer from the difficulty in fabrication of well-dispersed nickel oxide on the substrates. In practice, an electrode composed of nanosized materials is more difficult to fabricate due to the poor dispersibility of nanosized materials in slurry (composed of organic solvent, nanosized materials, polymer binder, and conducting agent, etc.). To alleviate such difficulties, EPD is proposed for fabricating well-dispersed nickel oxide electrodes.

EPD has been investigated as a preparation method for thin films of functional materials on different substrates [16–18]. In general, EPD proceeds via three processes: particle charging, particle transport under the applied electric field, and deposition of particles with neutralization [19]. Cathodic or anodic deposition can be achieved depending on the particle charge [17]. EPD may offer a simple approach to obtain an acceptable nickel oxide electrode

* Corresponding author. Fax: +886 9 45614423.
E-mail address: ms_wu@url.com.tw (M.-S. Wu).

0378-7753/$ – see front matter © 2008 Elsevier B.V. All rights reserved.
doi:10.1016/j.jpowsour.2008.10.049

because it has the advantages of short formation time, simple setup, low cost, and suitability for mass production. In addition, weight and thickness of the nickel oxide deposit may be easily controlled by varying the applied voltage difference, bath composition, and deposition time. Therefore, in this work, EPD is used to fabricate nanostructured nickel oxide electrode at room temperature without any template, and the obtained electrode is analyzed in its capacitive behavior.

2. Experimental

Nickel hydroxide powder was synthesized by chemical precipitation method. Nickel salt, 0.1 M $NiSO_4{\cdot}6H_2O$, and 28 wt.% NH_3 buffer solution were mixed and maintained at a pH value of 9.1 M NaOH solution was then added and stirred with the mixture in a beaker [4]. The precipitation was formed instantaneously. The green precipitation of the nickel hydroxide powder was filtered and washed with de-ionized water several times in order to remove any impurity. The precipitation was then dried at 100 °C for 3 h.

The film electrodes were obtained by dip-coating colloidal nickel hydroxide directly onto stainless steel (SS) foil. Nickel hydroxide powder (0.5 g) was added to an isopropyl alcohol solution (IPA, 50 ml) and mixed by ultrasonic vibrations for 1 h to form a homogeneous solution. Prior to coating, SS foil was polished with emery paper and rinsed by ultrasonic vibrations in acetone and de-ionized water, respectively. One side of the SS substrate was exposed, while the other side had been covered with a sheet of polymer insulator. Nickel hydroxide was coated on one side of the SS foil (2 cm × 2 cm) by dipping the foil into the homogeneous solution and withdrawing it at a controlled speed several times to obtain the required weight. After coating, resultant film was rinsed several times in de-ionized water and dried at 300 °C for 3 h in air to form nickel oxide electrode.

EPD bath was prepared by suspending IPA (50 ml), iodine (0.05 g), water (1.5 g), and nickel hydroxide powder (0.5 g) using the ultrasonic vibrations for 1 h to form a homogeneous solution. EPD of the nickel oxide electrode was carried out by applying a voltage difference of 10 V (Keithley, 2400 source meter, USA) between working (negative electrode, SS, 2 cm × 2 cm) and counter (positive electrode, platinum, 2 cm × 2 cm) electrodes for 30 s to obtain the required weight. One side of the SS substrate was exposed opposite a counter electrode, while the other side had been covered with a sheet of polymer insulator. The distance between working and counter electrodes was kept at 1 cm. After deposition, the deposited nickel hydroxide electrode was dried at 300 °C for 3 h in air to form nickel oxide electrode.

Electrochemical capacitive behavior of the nickel oxide electrode was determined by cyclic voltammetry in a three-electrode cell (beaker-type electrochemical cell) equipped with the working electrode, a platinum counter electrode, and a saturated Ag/AgCl reference electrode in 0.5 M KOH aqueous solution. The geometric surface area of a platinum counter electrode was 2 cm × 2 cm. The electrode was cycled at different scan rates using a potentiostat/galvanostat (CH Instruments, CHI 608, USA) in the potential range of −0.2 to 0.5 V versus a saturated Ag/AgCl reference electrode. Charge/discharge and cycle-life stability were performed by a source meter (Keithley 2400, USA) in the potential range of −0.2 to 0.5 V versus Ag/AgCl electrode at a current density of 4 A g^{-1}. All data acquisitions in Keithley 2400 were carried out through an interface (RS-232) with LabVIEW software. The amount of nickel oxide deposits for electrochemical tests was measured by a microbalance (Ohaus G160, USA) with an accuracy of 0.01 mg and was kept almost the same (about 0.45 mg) for each electrode by adjusting the deposition time. AC impedance measurements were conducted by means of a potentiostat (CH Instruments CHI 608, USA) under open-circuit condition. An AC perturbation amplitude of 10 mV versus the open-circuit potential was applied in the frequency range between 50 kHz and 0.1 Hz.

Specific surface area and average pore diameter of the nickel oxide powder after annealing at 300 °C for 3 h were measured by the Brunauer–Emmett–Teller (BET) technique (Micromeritics, ASAP 2010, USA) using N_2 gas. Surface morphology of the deposited nickel oxide films was examined with a field-emission scanning electron microscope (FESEM, Phillips, XL-40FEG, Holland) with an accelerating voltage of 15 keV. Crystal structure of the synthesized nickel oxide powder was identified by X-ray powder diffraction (XRD, Rigaku, MAX-2200, Japan) with a Cu Kα target (wavelength = 1.54056 Å). Diffraction data were collected for 1 s at each 0.04° step width over 2θ, ranging from 20° to 80°. The zeta potential of the nickel hydroxide suspension at different additives was measured by a zeta potential analyzer (Brookhaven, 90Plus, USA).

3. Results and discussion

Previous results indicated that an optimum annealing temperature of the nickel oxide/hydroxide nanoplatelets prepared by chemical precipitation is found to be about 300 °C in terms of electrode's capacitive behavior [4]. Therefore, the annealing temperature in this work is set at 300 °C for 3 h. Specific surface area and average pore diameter of the synthesized nickel oxide powder after annealing at 300 °C for 3 h are 170 $m^2\ g^{-1}$ and 6 nm, respectively, measured by BET method. BET analysis of the prepared electrodes is not shown here because it is difficult to deposit the requisite quantity of material needed for BET analysis (the amount of deposits is about 0.45 mg for each electrode). Crystal structure of the nickel oxide powder is identified by the XRD and the diffraction pattern is shown in Fig. 1. Diffraction peaks are indexed as cubic NiO (JCPDS 47-1049) with lattice parameters of a = 4.1771 Å and space group *Fm3m* (2 2 5). In addition, crystal structure of the nickel oxide electrodes fabricated by dip coating and EPD methods is similar to that of nickel oxide powder after heat treatment.

Fig. 2a shows the EPD current associated with time at different applied voltages in a suspension without iodine additive: suspension contains nickel hydroxide nanoplatelets (0.5 g), IPA (50 ml), and water (1.5 g). The depositing current is increased only

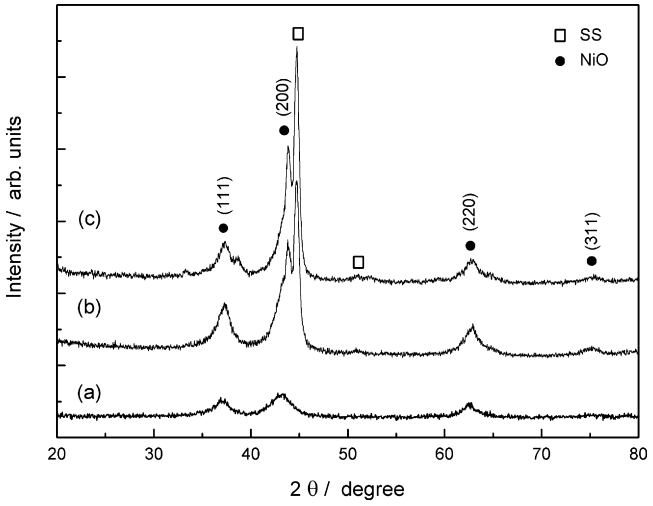

Fig. 1. XRD pattern of (a) synthesized nickel oxide powder and nickel oxide electrode deposited by (b) conventional dip coating and (c) proposed EPD methods after annealing at 300 °C for 3 h.

slightly by increasing the applied voltage. Even when the voltage is increased up to 200 V, the corresponding current is still very low. On the other hand, at low applied voltage for 300 s, nickel hydroxide deposit is observed neither on the negative electrode nor the positive electrode. At a high voltage of 200 V for 300 s, only a very small amount of nickel hydroxide deposit is observed on the positive electrode, meaning that the deposition rate is very slow. These results reveal that nickel hydroxide nanoplatelets in the IPA–water solution without iodine additive are negatively and weakly charged and move towards the positive electrode at high electric field. In general, the EPD current (deposition rate) and powder dispersion depend strongly on the zeta potential of the particles in a suspension. The zeta potential of the nickel hydroxide powder in the IPA suspension without additives is measured to be about −5 mV. Such small negative zeta potential is responsible for the low deposition rate. On the other hand, if the particles have a low magnitude of the zeta potential, the suspension is unstable because there is no significant repulsion force between particles to prevent the agglomeration of particles. As a result, a weakly charged nickel hydroxide is detrimental to the EPD in terms of deposition rate and powder dispersion.

Surface charge of the nickel hydroxide nanoplatelet, which can be controlled by addition of charging agent to the suspension, plays an important role in stabilization of the suspension as well as in deposition stage. Fig. 2b shows the EPD current associated with time at different applied voltages in a suspension with iodine and water additives. Obviously, the EPD current is significantly improved by using additives. The higher the applied voltage, the higher the EPD current. Nickel hydroxide deposit is significantly observed only on the negative electrode even at a low voltage of 5 V for 30 s. The zeta potential of the nickel hydroxide nanoplatelet is measured to be about 30 mV. Such high zeta potential is beneficial to the powder dispersion and facilitates powder deposition under an applied electric field. These results reveal that the nickel hydroxide nanoplatelets in an IPA solution containing iodine and water additives are positively charged and move towards the negative electrode under the applied field. In contrast with the nickel hydroxide of negatively charged surface, a reversal of the charge of nickel hydroxide particle can be achieved by adsorption of H^+ on the nickel hydroxide of negatively charged surface in the IPA bath with additives. Previous studies indicated that EPD in acetone bath, acetone generates the H^+ ion by the keto-enol reaction catalyzed by H_2O and I_2, and as a result the obtained H^+ ions are adsorbed on the particles resulting in positively charged particles [17,18]. It was established that more stable suspensions can be obtained in the IPA solvent when I_2–H_2O–acetone additive is used for particle charging [17]. In this work, an alternative procedure has also been used for nickel hydroxide charging based on the adsorption of H^+ ions on the surface of nickel hydroxide nanoplatelets. The H^+ ions may be generated by addition of I_2 and H_2O into to the IPA solvent according to the following reaction,

$$I_2 + H_2O \rightarrow H^+ + I^- + HOI \quad (1)$$

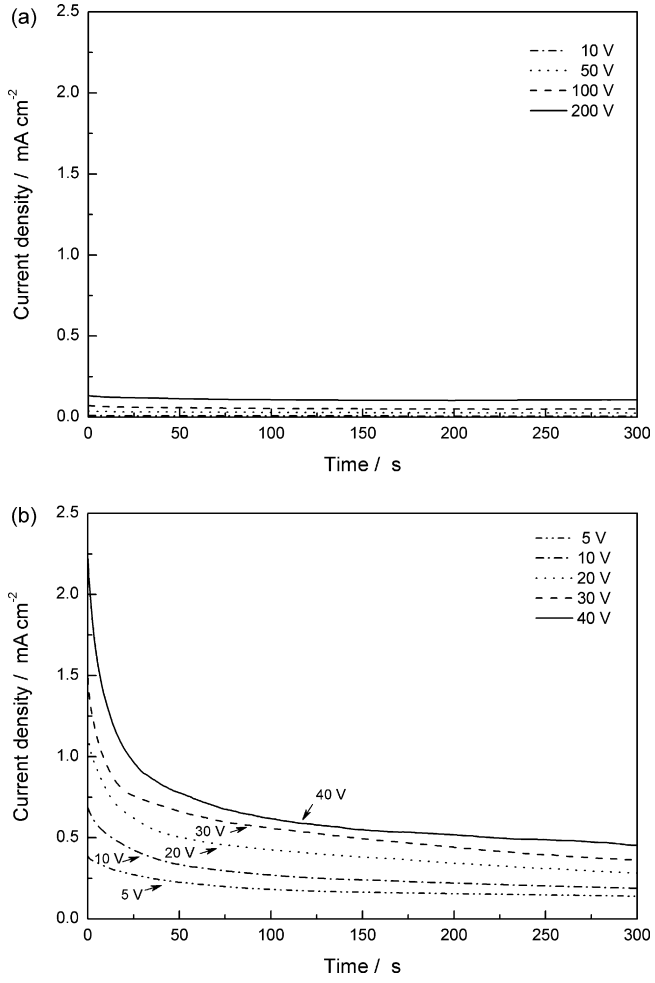

Fig. 2. Deposition-current density associated with time at different applied voltages during EPD in the IPA–water bath (a) without iodine additive and (b) with iodine additive.

Fig. 3 shows a schematic diagram of the proposed nickel hydroxide nanoplatelet deposition in the EPD process. H^+ ions are adsorbed by the nickel hydroxide nanoplatelets of negatively and weakly charged surface to form more positively charged nanoplatelets. EPD of the nickel hydroxide electrode is achieved via transport of positively charged nanoplatelets towards a negative electrode and deposition of nanoplatelets with neutralization under the applied electric field. Hydrogen evolution is accompanied during deposition by combination of the adsorbed H^+ ions on the surface of nickel hydroxide nanoplatelets. According to Koura et al. [18], the adsorbed H^+ ions on the oxide particle move to the surface of substrate by diffusion through a small opening in the oxide film according to the voltage gradient and the concentration, and subsequently discharge to emit hydrogen gas. As a result, the oxide particles continue to deposit on the oxide film. They concluded that the discharge of H^+ ions on the non-conductive oxide film surface is impossible [18]. In this work, however, the discharge of H^+ ions on the surface of nickel hydroxide film may be possible because the nickel hydroxide is electrically conducting compared with non-conductive oxides.

Fig. 4 shows the relationship between deposit weight and deposition time obtained for an applied voltage of 10 V in the IPA bath with water and iodine additives. Obviously, the deposit weight increases with EPD time; a nearly linear dependence is obtained, reflecting that this dependence allows for simple control of the deposition process.

Fig. 5 shows the surface morphology of nickel oxide electrode deposited by conventional dip coating and proposed EPD. All samples are heat-treated at 300 °C for 3 h, with the result that the nickel hydroxide deposit converts into nickel oxide. Obviously, the deposit prepared by conventional dip coating is not uniformly distributed on the SS substrate (Fig. 5a). Interestingly, when an electrode is fabricated by EPD, the surface of SS substrate is adherent and consisted of a relatively uniform nickel oxide distribution (Fig. 5b). SEM images in high magnification show that both deposited electrodes are porous and composed of nanoplatelets (Fig. 5c and d). In the duration of dip coating (suspension contains nickel hydrox-

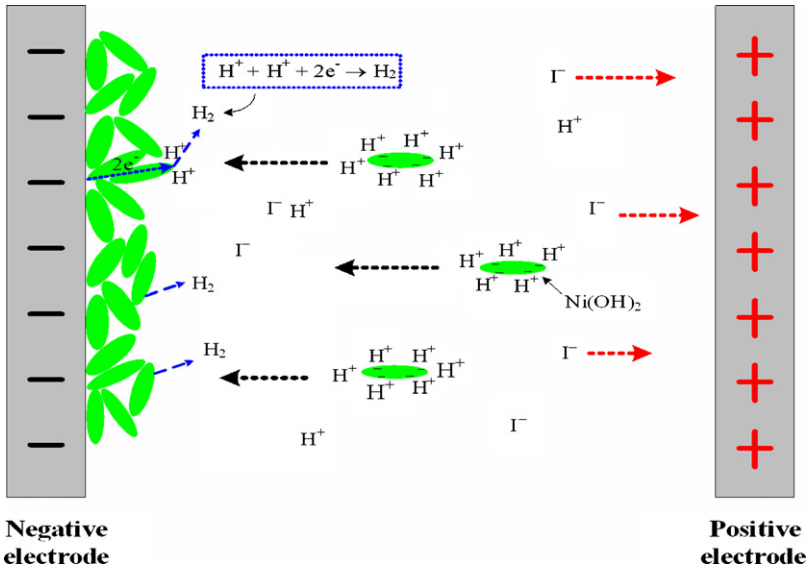

Fig. 3. Schematic diagram of the proposed nickel hydroxide nanoplatelet deposition in the EPD process.

ide, IPA, and water), when ultrasonic treatment is interrupted, the weakly charged nickel hydroxides in the suspension tend to aggregate owing to an insufficient repulsion force between nanoplatelets (the zeta potential is about −5 mV). In contrast, H^+ ions adsorbed on the nickel hydroxide forming a more positive zeta potential (about 30 mV) may prevent the agglomeration of nanoplatelets due to an increased repulsion force between nanoplatelets in the suspension. Therefore, a well-dispersed nickel oxide electrode prepared by EPD method is obtained.

Cyclic voltammogram (CV) is generally used to investigate the capacitive behavior of an electrode material. In an ideal electrical double-layer capacitor containing flat electrodes, the CV current response shows a rectangular mirror image with respect to the zero-current line, and it also shows a rapid current response on the potential reversal at each end potential [20,21]. Generally, the electrical double-layer capacitance is independent of the scan rate and potential [21]. When Faradaic reaction and Ohmic resistance (resulting from electrolyte diffusion within porous electrode) are involved, the rectangular mirror image is no longer maintained [21].

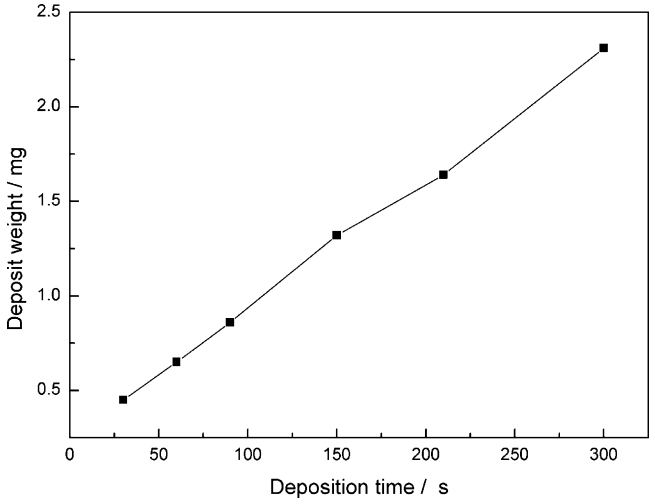

Fig. 4. Relationship between deposit weight and deposition time obtained for an applied voltage of 10 V in the IPA bath with water and iodine additives.

Fig. 6 shows the CVs of nickel oxide electrodes prepared by dip coating and EPD at a scan rate of 10 mV s^{-1}. In order to investigate the Faradaic capacitance of nickel oxide materials, the potential window was usually set at a range of 0–0.5 V versus Ag/AgCl reference electrode. Our previous work indicated that the specific capacitance of nickel oxide electrode comes from both the faradic and the electrical double-layer capacitances [10]. Results revealed that when the applied potential is more negative than 0.1 V, the specific capacitance of nickel oxide electrode comes mainly from the electrical double-layer capacitance. Therefore, in this work, in order to show the electrical double-layer capacitance of the prepared nickel oxide electrodes in the potentials negative than 0 V, a lower limit potential was set at −0.2 V. The upper limit potential was set at 0.5 V. Consequently, a potential range of −0.2 to 0.5 V was used to investigate the capacitive behavior of nickel oxide electrodes. Deposit weight for each film electrode is held almost the same. Film thickness was obtained from the cross-sectional images of the films. The related images are not shown here. Film thicknesses of the NiO electrodes fabricated by EPD and dip-coating methods were measured to be about 200 nm and 240 nm, respectively.

Generally, specific capacitance of an ideal electrical double-layer capacitor is independent of the potential, while specific capacitance of an electrochemical capacitor (redox capacitor) depends significantly on the potential. In order to investigate the effect of potential on the specific capacitance of electrodes, specific capacitance is, therefore, used instead of the current in Fig. 6. Specific capacitance in response to the potential can be calculated according to the following equation:

$$C = \frac{i}{\nu \cdot w} \tag{2}$$

where C is the specific capacitance of active material (F g^{-1}), w is the mass of active material (g), ν is the scan rate (V s^{-1}), i is the cathodic or anodic current (A). Clearly, specific capacitance of the deposited nickel oxide electrodes depends on the scanned potential. The CV shape of electrode prepared by dip coating is similar to that of prepared by EPD at a scan rate of 10 mV s^{-1}, electrodes show a roughly mirror image with respect to the zero-capacitance line, also show a rapid capacitance response on the potential reversal at each end potential, a representation of capacitive behavior. Interestingly, an electrode prepared by EPD has higher capacitance

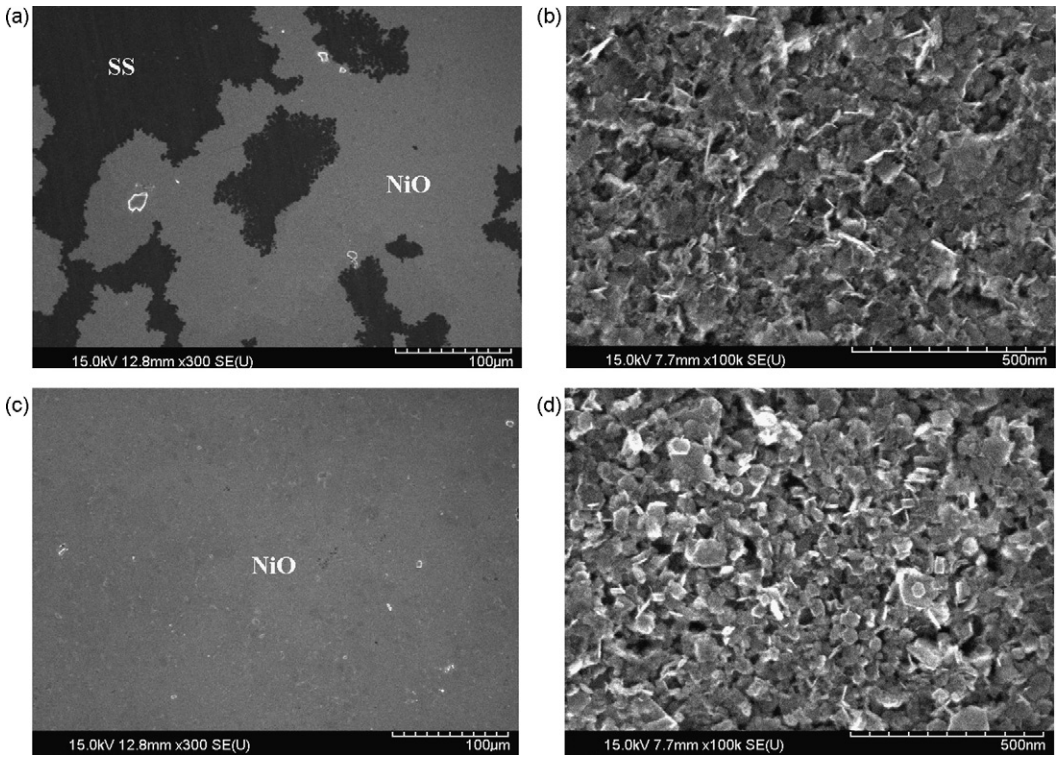

Fig. 5. Surface morphology of the nickel oxide electrode deposited by (a) conventional dip coating and (b) proposed EPD methods. Images in high magnification for the electrodes deposited by dip coating and EPD are shown in (c) and (d), respectively.

response than one prepared by dip coating in the scanned potential window.

There are two pairs of redox peaks (O1/R1 and O2/R2) observed in Fig. 6. These redox peaks may presumably come from the redox processes of nickel oxide (NiO/NiOOH) and of nickel hydroxide ($Ni(OH)_2$/NiOOH) [22]. CV curve of blank SS substrate (after heating at 300 °C for 3 h) in 0.5 M KOH aqueous solution, which is not shown here, was scanned for comparison; capacitance is very low. Conclusively, capacitance comes mainly from the nickel oxide electrode instead of the SS substrate.

In order to alleviate the oxygen evolution at higher anodic potentials, the positive limit potential used in CV scans is set at 0.5 V versus Ag/AgCl. As seen from Fig. 6, when the positive limit potential is lower than 0.1 V, the CVs show a rectangular mirror image with respect to the zero-capacitance line, which represents an electrical double-layer capacitive behavior, specific capacitance of the electrode prepared by EPD method in a potential range of −0.2 to 0.1 V is about 80 F g^{-1}. When the positive limit potential is higher than 0.1 V, the CVs include the Faradaic behavior. Through redox reactions, much higher specific capacitance (larger than 110 F g^{-1}) can be stored in a Faradaic capacitor than in a double-layer capacitor.

Fig. 7 shows the CVs of nickel oxide electrodes prepared by dip coating and EPD at different scan rates. In general, scan rate influences the specific capacitance of an electrochemical capacitor rather than an ideal double-layer capacitor [21]. An electrochemical capacitor, due to the Faradaic reaction and Ohmic resistances, has a lower specific capacitance when the scan rate is high. High scan rate in CV scan corresponds to the high-rate charge/discharge (galvanostatic). Current response shown in Fig. 7 is increased proportionally by increasing the scan rate. In addition, two redox peaks are also found in the CV curves indicating that the redox capacitance contributes to the measured capacitance of the capacitor even at high rates.

An electrode prepared by EPD at all CV scan rates shows a roughly mirror image with respect to the zero-current line and a rapid current response on the potential reversal at each end potential, independent of scan rate; the CV shape represents a capacitive behavior at high scan rates (Fig. 7b). As seen from Fig. 7a, a roughly mirror image of the CV curve is no longer maintained at higher scan rates, especially at anodic scan beginning at −0.2 V. Average specific capacitance at various scan rates is calculated by Eq. (2). Note that i is the average cathodic or anodic current (A) in Eq. (2). The relationship between average specific capacitance and scan rate of the deposited nickel oxide electrodes at various scan rates is therefore investigated, and Fig. 8 shows the results. Clearly, both electrodes have higher average specific capacitance at low scan rate than that at high scan rate. An electrode prepared by

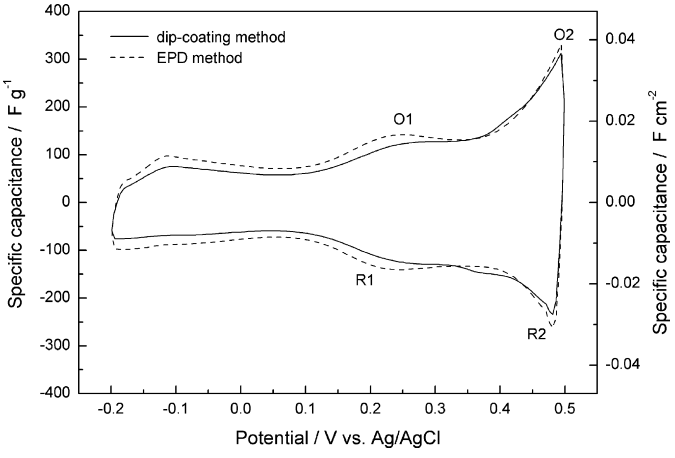

Fig. 6. CV s of the nickel oxide electrodes prepared by dip coating and EPD methods at a scan rate of 10 mV s^{-1}.

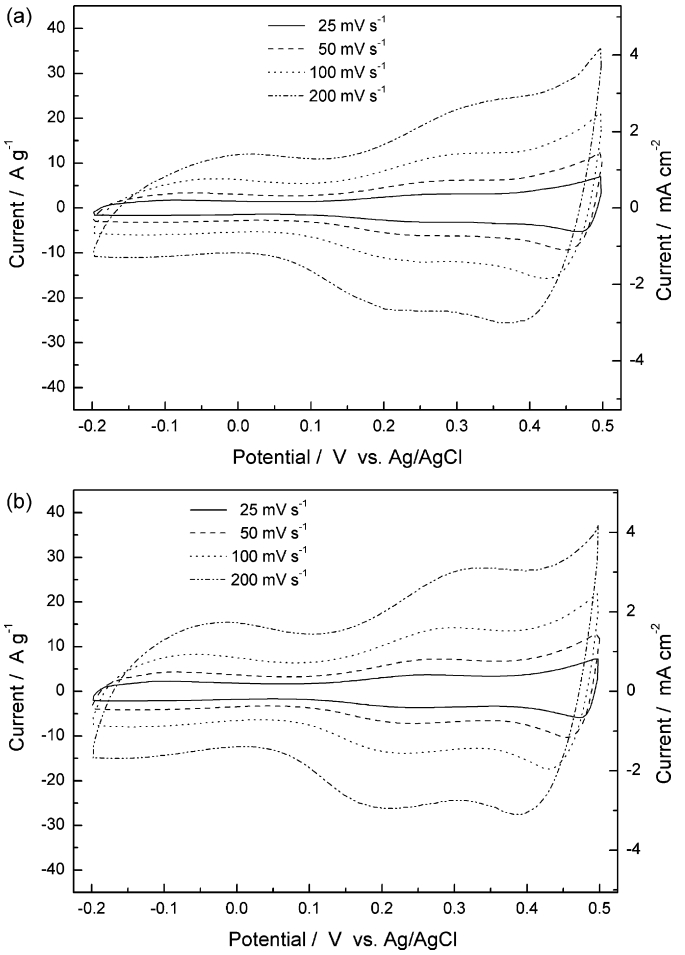

Fig. 7. CVs of the nickel oxide electrodes prepared by (a) dip coating and (b) EPD methods at different scan rates.

EPD has an average specific capacitance of 112 F g^{-1} at a low scan rate of 10 mV s^{-1}, and the value reduces slightly to 80 F g^{-1} (72% capacitance of 10 mV s^{-1}) at a high scan rate of 500 mV s^{-1}. The high-capacitance retention at high scan rate also reflects that the Faradaic reaction on the surface of deposited nickel oxide is fast enough to maintain the current response during high-rate scanning. The relatively small decrease in specific capacitance with increasing scan rate indicates the high-power characteristics of the nickel oxide electrode. Possibly, this is a result of nanoporous-structure: large electroactive area for fast redox reactions, and shortened diffusion paths for high-rate charge/discharge. On the other hand, specific capacitance value of the electrode prepared by dip coating is lower than that of prepared by EPD at all scan rates. Possibly, this is a result of non-uniform distribution of the aggregated nickel oxides on the SS substrate. Comparing with previous literatures, a specific capacitance of 112 F g^{-1} of the nickel oxide electrode at a CV scan rate of 10 mV s^{-1} is higher than that obtained from chemical precipitation, but somewhat lower than that obtained from electrochemical deposition. Liu et al. [23] have reported an electrochemical capacitor using nickel oxide prepared by chemical precipitation method; a specific capacitance of 65 F g^{-1} was obtained. A less expensive, more controllable electrochemical method of preparing porous nickel oxide capacitors was reported by Srinivasan et al., a specific capacitance of 59 F g^{-1} based on a device fabricated from two identical nickel oxide electrodes was obtained at slow scan rate of 20 mV s^{-1} [22]. Recently, a higher specific capacitance of nickel oxide has been reported: nanoarrays with ordered mesoporous structure (capacitance of 120 F g^{-1}) were synthesized by calcining nickel nitrate at 550 °C within a silica template [24]; three-dimensional nanowhiskers prepared by potentiodynamically depositing nickel hydroxide (nickel chloride plating bath) on SS and heating in air at 300 °C for 3 h has a capacitance of 138 F g^{-1} [9]. This work does not aim to obtain a high specific capacitance, but to develop the nickel oxide electrode of high uniformity for high-rate applications. EPD method turns out to have positive effects on the capacitive behavior of nickel oxide electrode. Therefore, the proposed EPD method provides a potential process for fabricating electrodes.

Fig. 9 shows the Nyquist plots of the nickel oxide electrodes fabricated by dip coating and EPD methods. The corresponding equivalent circuit for impedance analysis is displayed in the inset of Fig. 9. At very high frequencies, the intercept at real part (Z') is a combinational resistance of ionic resistance of electrolyte, intrinsic resistance of substrate, and contact resistance at the active material/current collector interface (R_e) [25]. This value is almost the same for both electrodes. A major difference is the semicircle in the high-frequency range shown in the inset of Fig. 9, which corresponds to the charge-transfer resistance (R_{ct}) caused by the Faradaic reactions and the double-layer capacitance (C_{dl}) on the grain surface. Charge separation at micropores is represented by the

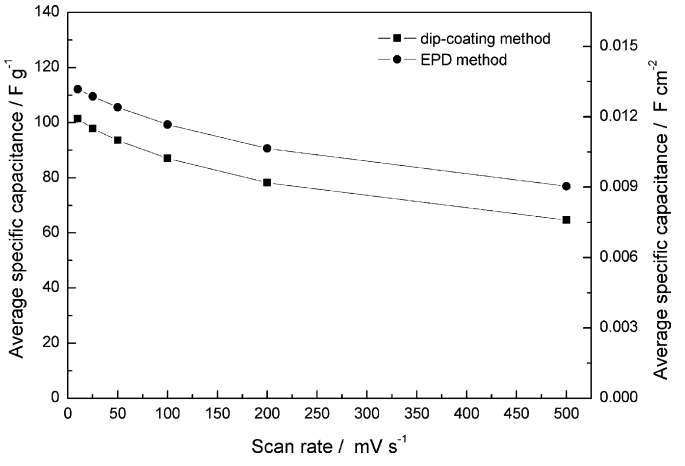

Fig. 8. Relationship between the average specific capacitance and scan rate of the deposited nickel oxide electrodes.

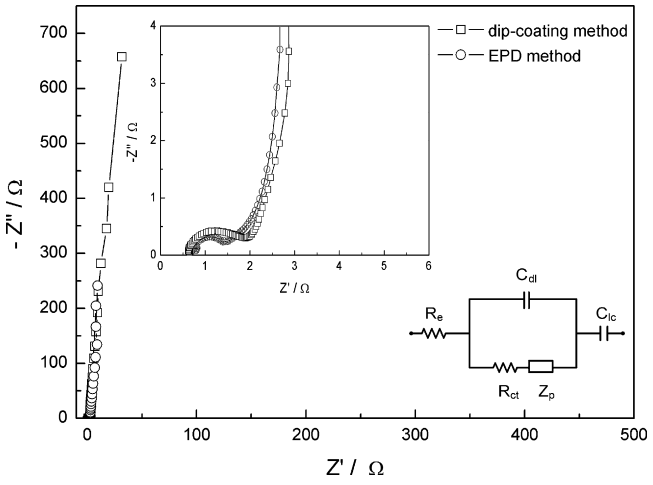

Fig. 9. Nyquist plots of the nickel oxide electrodes fabricated by dip coating and EPD methods.

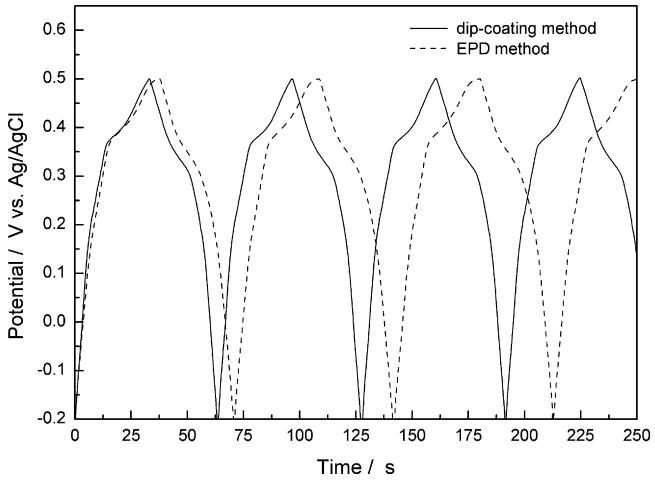

Fig. 10. Galvanostatic charge/discharge curves of the nickel oxide electrodes prepared by dip coating and EPD methods at a current density of $4\,A\,g^{-1}$.

transmission line Z_p which relates to the distributed electronic and ionic conductivity and double-layer capacitance inside the micropores; C_{lc} is the limit capacitance [26]. The calculated charge-transfer resistances for the electrodes fabricated by dip coating and EPD methods are about 1.5 Ω and 1.0 Ω, respectively. The higher the charge-transfer resistance, the lower the specific capacitance of the electrode. The nickel oxide electrode prepared by EPD strategy has a lower charge-transfer resistance reflecting a higher specific capacitance due to the well-dispersed nickel oxide electrode.

Fig. 10 shows the galvanostatic charge/discharge curves of nickel oxide electrodes prepared by EPD and dip coating at a current density of $4\,A\,g^{-1}$. Total time for charging (from −0.2 to 0.5 V) and discharging (from 0.5 to −0.2 V) processes are almost the same. Similar time length implies a high reversibility of the Faradaic reaction on the surface of nickel oxide grains, which is in good agreement with the CV results. Specific capacitance of an electrode during galvanostatic test can be calculated according to the following equation:

$$C = \frac{i \cdot \Delta t}{w \Delta V} \tag{3}$$

where w is the mass of active material, ΔV is the potential window, i is the discharge current applied for time Δt. Fig. 11 shows the relationship between the capacitance retention and cycle number during galvanostatic charging and discharging. Cycle-life stability is carried out by galvanostatic charge/discharge cycling at a current density of $4\,A\,g^{-1}$. Capacitance retention of the electrode prepared by EPD shows excellent stability because there is very little degradation of the specific capacitance after 5000 test cycles, approximately 90%. The electrode has a stable capacitance during cycling, and therefore, is suitable for long-time capacitor applications in KOH solution.

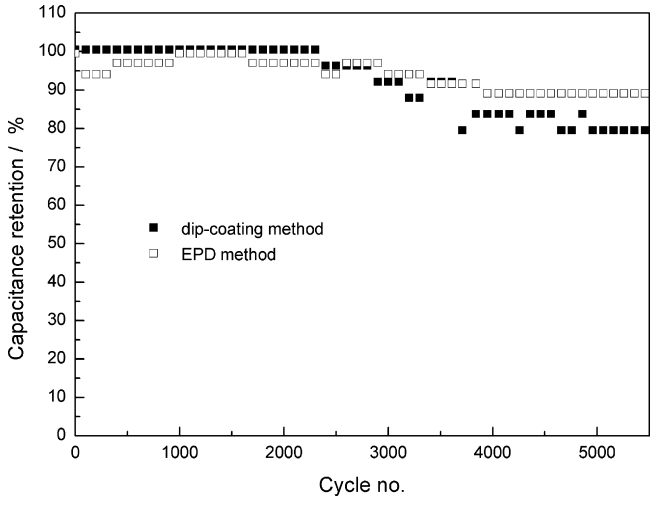

Fig. 11. Relationship between the capacitance retention and cycle number during galvanostatic charging and discharging.

4. Conclusion

Nickel hydroxide particle of weakly charged surface is detrimental to EPD and dispersion resulting in a very low deposition rate. When adding iodine into IPA–water suspension, hydrogen ions are generated by the reaction between iodine and water and then adsorbed on the particle forming more positively charged particle (the zeta potential is about 30 mV), leading to an increase in EPD current. Nickel oxide nanoplatelets of weakly charged surface are not uniformly distributed on the substrate by conventional dip-coating method. Possibly, this is due to the agglomeration of nanoplatelets. In contrast, H^+ ions adsorbed on the nickel hydroxide resulting in a more positive zeta potential can mitigate the agglomeration of nanoplatelets due to an increased repulsion force between nanoplatelets. Interestingly, an electrode prepared by EPD method has a higher specific capacitance than one prepared by dip-coating method at all CV scan rates. In addition, the relatively small decrease in specific capacitance with increasing scan rate indicates the high-power characteristics of deposited nickel oxide electrode. Electrode prepared by EPD also shows excellent stability because there is very little degradation of the specific capacitance after 5000 test cycles. Capacitive behavior of the electrode prepared by EPD is superior to that prepared by dip coating. This is attributed to the well-dispersed nickel oxide electrode fabricated by EPD with iodine and water additives.

Acknowledgment

The authors gratefully acknowledge financial support from the National Science Council, Taiwan, Republic of China (Project No. NSC 97-2221-E-151-029).

References

[1] J.P. Zheng, T.R. Jow, J. Electrochem. Soc. 142 (1995) L6.
[2] J.P. Zheng, P.J. Cygan, T.R. Jow, J. Electrochem. Soc. 142 (1995) 2699.
[3] M.W. Xu, S.J. Bao, H.L. Li, J. Solid State Electrochem. 11 (2007) 372.
[4] M.S. Wu, H.H. Hsieh, Electrochim. Acta 53 (2008) 3427.
[5] V. Srinivasan, J.W. Weidner, J. Electrochem. Soc. 147 (2000) 880.
[6] E.E. Kalu, T.T. Nwoga, V. Srinivasan, J.W. Weidner, J. Power Sources 92 (2001) 163.
[7] K.W. Nam, W.S. Yoon, K.B. Kim, Electrochim. Acta 47 (2002) 3201.
[8] K.W. Nam, E.S. Lee, J.H. Kim, Y.H. Lee, K.B. Kim, J. Electrochem. Soc. 152 (2005) A2123.
[9] K.R. Prasad, N. Miura, Appl. Phys. Lett. 85 (2004) 4199.
[10] M.S. Wu, Y.A. Huang, C.H. Yang, J.J. Jow, Int. J. Hydrogen Energy 32 (2007) 4153.
[11] M.S. Wu, Y.A. Huang, C.H. Yang, J. Electrochem. Soc. 155 (2008) A798.
[12] C. Du, N. Pan, Nanotechnology 17 (2006) 5314.
[13] C. Du, N. Pan, J. Power Sources 160 (2006) 1487.
[14] J.H. Jang, K. Machida, Y. Kim, K. Naoi, Electrochim. Acta 52 (2006) 1733.
[15] J.H. Jang, A. Kato, K. Machida, K. Naoi, J. Electrochem. Soc. 153 (2006) A321.
[16] W. Sugimoto, K. Yokoshima, K. Ohuchi, Y. Murakami, Y. Takasu, J. Electrochem. Soc. 153 (2006) A255.
[17] I. Zhitomirsky, Mater. Lett. 37 (1998) 72.
[18] N. Koura, T. Tsukamoto, H. Shoji, T. Hotta, Jpn. J. Appl. Phys. 34 (1995) 1643.
[19] K. Kanamura, A. Goto, J.I. Hamagami, T. Umegaki, Electrochem. Solid-State Lett. 3 (2000) 259.
[20] H.Y. Lee, J.B. Goodenough, J. Solid State Chem. 144 (1999) 220.

[21] B.E. Conway, J. Electrochem. Soc. 138 (1991) 1539.
[22] V. Srinivasan, J.W. Weidner, J. Electrochem. Soc. 144 (1997) L210.
[23] K.C. Liu, M.A. Anderson, J. Electrochem. Soc. 143 (1996) 124.
[24] Y.G. Wang, Y.Y. Xia, Electrochim. Acta 51 (2006) 3223.
[25] J. Gamby, P.L. Taberna, P. Simon, J.F. Fauvarque, M. Chesneau, J. Power Sources 101 (2001) 109.
[26] A.D. Fabio, A. Giorgi, M. Mastragostino, F. Soavi, J. Electrochem. Soc. 148 (2001) A845.